Nonlinear Dynamics and Chaos: part 2: Two-Dimensional Flows: Ch 8: Bifurcations Revisited

Charlie Seager

4/25/2024

Chapter 8.0 Inroduction

This chapter extends our earlier work on bifurcations (Chapter 3). As we moe up from one-dimensional to two-dimensional systems, we still find that fixed points can be created or destoryed or destabilized as parameters are varied-but now the same is true of closed orbits as well. Thus we can begin to describe the ways in which oscillations can be tunred on or off.

In this broader context, what exactly do we mean by a bifurcation? The usual definition involves the concept of "topological equivalence" (Section 6.3): if the phase portrait changes its topological structure as a parameter is varied, we say that a bifurcation has occured. Examples include changes as the number or stability of fixed points, closed orbits, or saddle connections as a parameter is varied.

This chapter is organized as follows: for each bifurcation, we start with a simple prototypical example, and then graduate to more challanging examples, either briefly or in seperate sections. Models of genetic switches, chemical oscillators, driven pendula and Josephson Junctions are used to illustrate the theory.

Chapter 8.1 Saddle-Node, Transcritical, and Pitchfork Bifurcations

The bifurcations of fixed points discussed in Chapter 3 have analogs in two dimensions (and indeed, in all dimensions). Yet it turns out that nothing really new happens when more dimensions are added-all the action is confined to a one-dimensional subspace along which the bifurcations occur, while in the extra dimensions the flow is either simple attraction or repulsion from the subspace, as we'll see below.

Saddle-Node Bifurcation

The saddle-node bifurcation is the basic mechanism for the creation and destruction of fixed points. Here's the prototypical example in two dimensions

$$\dot{x} = \mu - x^2$$
$$\dot{y} = -y \qquad (1)$$

In the x-direction we see the bifurcation behavior discussed in Section 3.1, while

in the y-direction the motion is exponentially damped.

Consider the phase portrait, as μ varies. For $\mu > 0$, figure 8.1.1 shows that there are two fixed points, a stable node at $(x*, y*) = (\sqrt{\mu}, 0)$ and a saddle at $(-\sqrt{\mu}, 0)$. As μ decreases, the saddle and node approach each other, then collide when $\mu = 0$ and finally disappear when $\mu < 0$

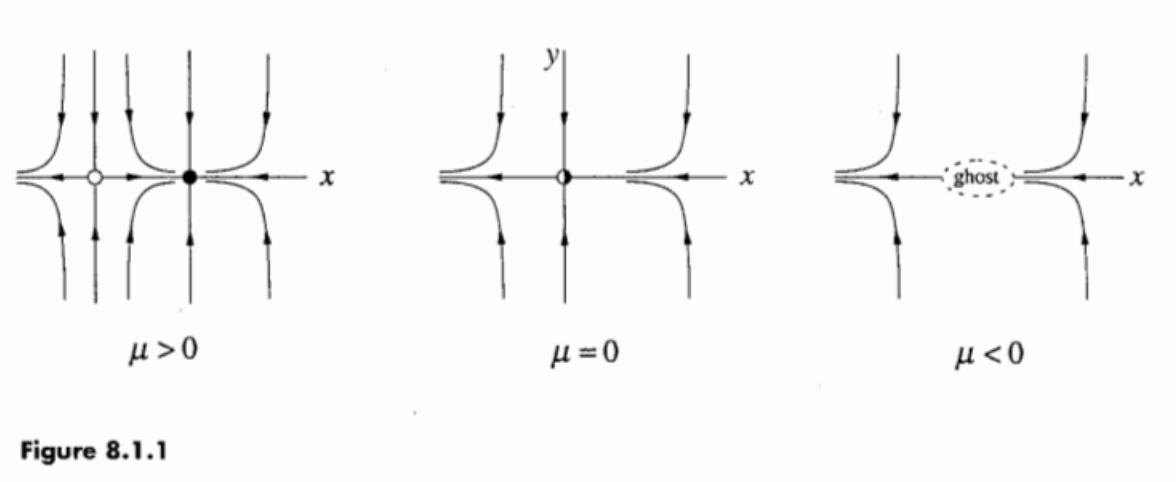

Figure 8.1.1

Even after the fixed points have annihibilated each other, they continue to influence the flow-as in Section 4.3, they leave a ghost, a bottleneck region that sucks trajectories in and delays them before allowing passage out on the other side. For the same reasons as in Section 4.3, the time spent in the bottleneck generically increases as $(\mu - \mu_c)^{-1/2}$, where μ_c is the value at which the saddle-node bifurcation occurs. Some applications of this scaling law in condensed matter physics are discussed by Strogratz and Westervelt (1989).

Figure 8.1.1 is representative of the following more general situation. Consider a two-dimensional system $\dot{x} = f(x, y), \dot{y} = g(xy)$ that depends on a parameter μ. Suppose that for some value of μ the nullclines intersect as shown in Figure 8.1.2. Notice that each intersection corresponds to a fixed point since $\dot{x} = 0$ and $\dot{y} = 0$ simultaneously. Thus, to see how the fixed ponits move as μ changes, we just have to watch the intersections. Now suppose that the nullclines pull away from each other as μ varies, becoming tangent at $\mu = \mu$. Then the fixed points approach each other and collide when $\mu = \mu_c$; after the nullclines pull apart, there are no intersections and the fixed points disappear with a bang. The point is that all saddle-node bifurcations have this character locally.

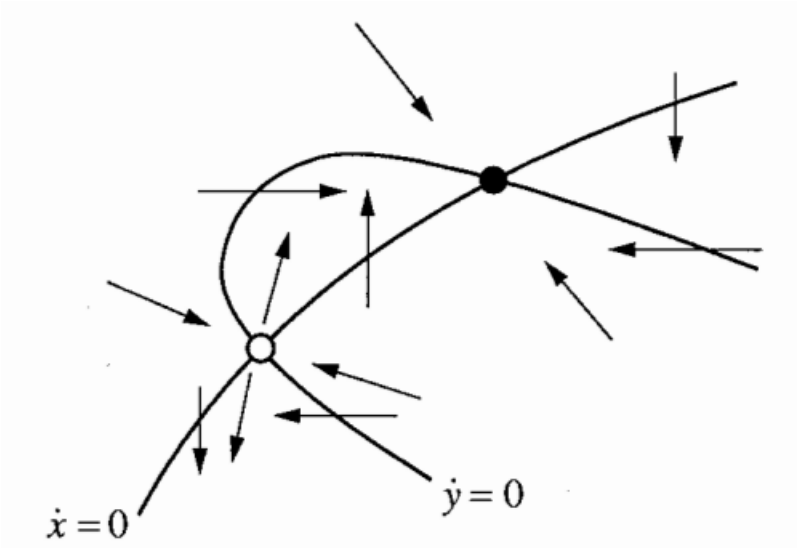

Figure 8.1.2

Transcritical and Pitchfork Bifurcations

Using the same idea as above, we can also construct prototypical examples of transcritical and pitchfork bifurcations at a stable fixed point. In the x-direction the dynamics are given by the normal forms discussed in Chapter 3, and in the y-direction the motion is exponentially damped. This yieds the following examples

$$\dot{x} = \mu x - x^2, \qquad \dot{y} = -y \text{ (transcritical)}$$
$$\dot{x} = \mu x - x^3, \qquad \dot{y} = -y \text{ (supercritical pitchfork)}$$
$$\dot{x} = \mu x + x^3, \qquad \dot{y} = -y \text{ (subcritical pitchfork)}$$

The analysis in each case follows the same pattern, so we'll discuss only the supercritical pitchfork, and leave the other two cases as excercises.

Chapter 8.2 Hopf Bifurcations

Suppose a two-dimensional system has a stable fixed point. What are all the possible ways it could lose stability as a parameter μ varies? The eigenvalues of the Jacobian are the key. If the fixed point is stable, the eigenvalues λ_1, λ_2 must both lie in the left half plane $Re\lambda < 0$. Since the λ's satisfy a quadratic equation with real coefficients, there are two possible pictures: either the eigenvalues are both real and negative (Figure 8.2.1a) or they are complex conjugates (Figure 8.2.1b). To destabalize the fixed point, we need one or both of the eigenvalues to cross into the right half-plane as μ varies

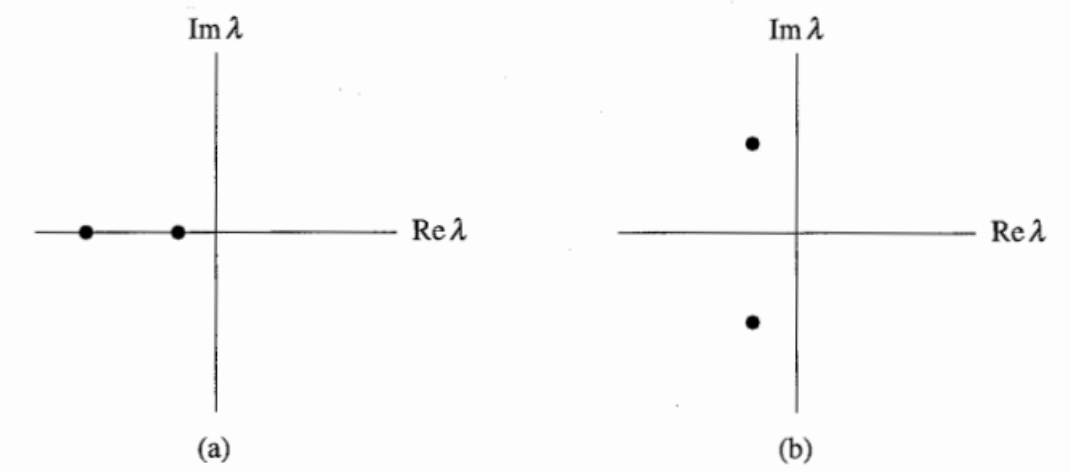

Figure 8.2.1

In Section 8.1 we explored the cases in which a real eigenvalue passes through $\lambda = 0$. These were just our old friends from Chapter 3, namely the saddle-node transcritical and pitchfork bifurcations. Now we consider the other possible scenario, in which two complex conjugate eigenvalues simultaneously cross the imaginary axis into the right half plane. **Supercritical Hopf Bifurcation**

Suppose we have a physical system that settles down to equilibrium through exponentially damped oscillations. In other words, small disturbances decay after "ringing" for a while (Figure 8.2.2a). Now suppose that the decay rate depends on a control parameter μ. If the decay becomes slower and slower and finally changes to growth at a critical value μ_c, the equilibrium state will lose stability. In many cases the resulting motion is a small amplitude, sinusoidal, limit cycle oscillation about the former steady state (Figure 8.2.2b). Then we say that the system has undergone a supercritical Hopf bifurcation.

In terms of the flow in phase space, a supercritical Hopf bifurcation occurs when a stable sprial changes into an unstable spiral changes into an unstable spiral surrounded by a small, nearly elliptical limit cycle. Hopf bifurcations can occur in phase spaces of any dimension $n \geq 2$, but as in the rest of this chapter, we'll restrict ourselves to two dimensions.

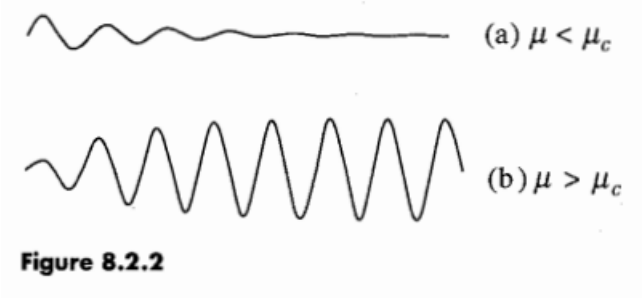

Figure 8.2.2

A simple example of a supercritical Hopf bifurcation is given by the following system:

$$\dot{r} = \mu r - r^3$$
$$\dot{\theta} = \omega + br^2$$

There are three paramters: μ controls the stability of the fixed point at the origin ω gives the frequency of infinitesimal oscillations, and b determines the dependence of frequency on amplitude oscillations.

Figure 8.2.3 plots the phase portraits for μ above and below the bifurcation. When $\mu < 0$ the origin r=0 is a stable spiral whose sense of rotation depends on the sign of ω. For $\mu = 0$ the origin is still a stable spiral, though a very weak one: the decay is only algebraically fast. (This case was shown in Figure 6.3.2. Recall that the linearization wrongly predicts a center at the origin.) Finally, for $\mu > 0$ there is an unstable spiral at the origin and a stable circular limit cycle at $r = \sqrt{\mu}$.

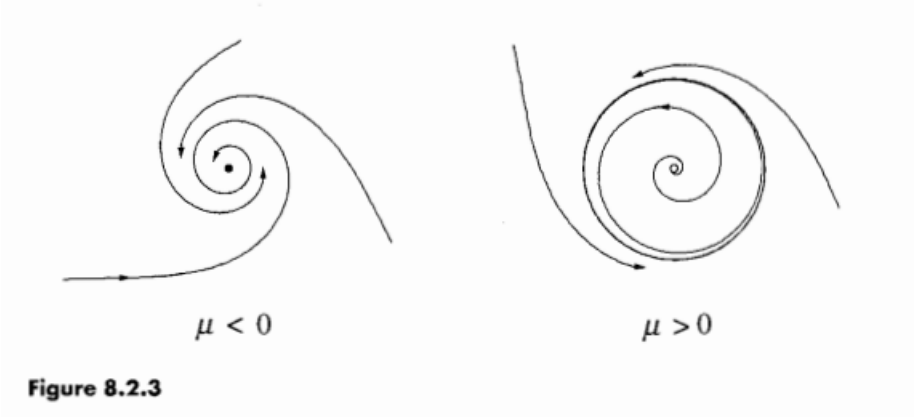

Figure 8.2.3

To see how the eigenvalues behave during the bifurcation, we rewrite the system in Cartesian coordinates: this makes it easier to find the Jacobian. We write $\dot{x} = rcos\theta$, $y = rsin\theta$. Then

$$\begin{aligned}\dot{x} &= rcos\theta - r\dot{\theta}sin\theta \\ &= (\mu r - r^3)cos\theta - r(\omega + br^2)sin\theta \\ &= (\mu - [x^2 + y^2])x - (\omega + b[x^2 + y^2])y \\ &= \mu x - \omega y + \text{cubic terms}\end{aligned}$$

and similarily

$$\dot{y} = \omega x + \mu y + \text{cubic terms.}$$

So the Jacobian at the origin is $A = \begin{pmatrix} \mu & -\omega \\ \omega & \mu \end{pmatrix}$ which has eigenvalues

$$\lambda = \mu \pm i\omega.$$

As expected, the eigenvalues cross the imaginary axis from left to right as μ increases from negative to positive values.

Rules of Thumb

Our idealized case illustrates two rules that hold generically for supercritical Hopf Bifurcations:

1. The size of the limit cycle grows continuously from zero, and increases

proportional to $\sqrt{\mu - \mu}$, for μ close to μ_c.

2. The frequency of the limit cycle is given approximately by $\omega = lim\lambda$, evaluated at $\mu = \mu_c$. This formula is exact at the birth of the limit cycle, and correct within $O(\mu - \mu_c)$ for μ close to μ_c. The period is therefore $T = (2\pi/Im\lambda) + O(\mu - \mu_c)$.

But our idealized example also has some artifactual properties. First, in Hopf bifurcations encountered in practice, the limit cycle is elliptical, not circular, and its shape becomes distorted as μ moves away from the bifurcation point. Our example is only typical topologically, not geometrically. Second, in our idealized case the eigenvalues move on horizontal lines as μ vaires, i.e., $Im\lambda$ is strictly independent of μ. Normally, the eigenvalues would follow a curvy path and cross the imaginary axis with nonzero slope (Figure 8.2.4).

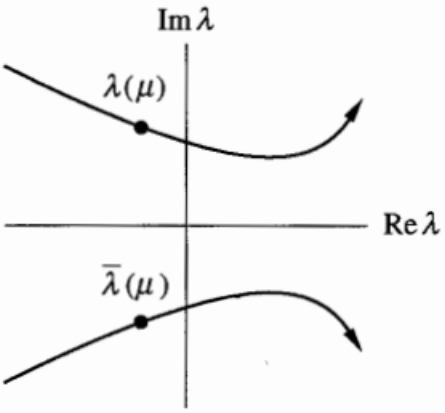

Figure 8.2.4

Subcritical Hopf Bifurcation

Subcritical Hopf Bifurcation

Like pitchfork bifurcations. Hopf bifurcations come in both super- and subcritical varieties. The subcritical case is always much mor edramatic, and potentially dangerous in engineering applciations. After the bifurcation, the trajectories must jump to a distant attractor, which may be a fixed point, another limit cycle, infinity, or-in three and higher dimensions-a chaotic attractor. We'll see a concrete example of this last, most interesting case when we study the Lorenz equations (Chapter 9)

But for now, consider the two-dimensional example

$$\dot{r} = \mu r + r^3 - r^5$$
$$\dot{\theta} = \omega + br^2$$

The important difference from the earlier supercritical case is that the cubic term r^3 is now destabilizing: it helps to drive trajectories away from the origin.

The phase portraits are shown in Figure 8.2.5. For $\mu < 0$ there are two attractors, a stable limit cycle and a stable fixed point at the origin. Between

them lies an unstable cycle, shown as a dashed curve in Figure 8.2.5; it's the player to watch in this scenario. As μ increases, the unstable cycle tightens, like a noose around the fixed point. A subcritical Hopf bifurcation occurs at $\mu = 0$, where the unstable cycle shrinks to zero amplitude and engulfs the origin, rendering it unstable. For $\mu > 0$, the large amplitude limit cycle is suddenly the only attractor in town. Solutions that used to remain near the origin are now forced to grow into large-amplitude oscillations.

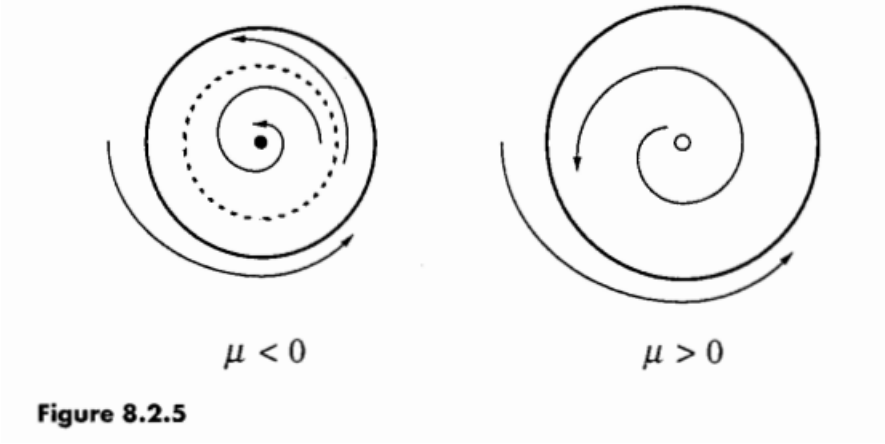

Figure 8.2.5

Note that the system exhibits hysteresis: once large-amplitude oscillations have begun, they cannot be turned off by bringing μ back to zero. In fact, the large oscillations will persist until $\mu = -1/4$ where the stable and unstable cycles collide and annihilate. The destruction of the large-amplitude cycle occurs via another type of bifurcation, to be discussed in section 8.4.

Subcritical Hopf bifurcations occur in the dynamics of nerve cells (Rinzel and Ermentrout 1989), in aeroelastic flutter and other vibrations of airplane wings (Dowell and Ilgamova 1988, Thompson and Stewart 1986) and in instabilities of fluid flows (Drazin and Reid 1981). **Subcritical, Supercritical or Degenerate Bifurcation?**

Given that a Hopf bifurcation occurs, how can we tell if its sub-or supercritical? The linearization doesn't provide a distinction: in both cases, a pair of eigenvalues moves from the left to the right half-plane.

An analytical criterion exists, but it can be difficult to use (see Excercises 8.2.12-15 for some tractable cases). A quick and dirty appraoch is to use the computer. If a small, attracting limit cycle appears immediately after the fixed point goes unstable, and if its amplitude shrinks back to zero as the parameter is reversed, the bifurcation is supercritical; otherwise it's probably subcritical, in which case the nearest attractor might be far from the fixed point, and the system may exhibit hysteresis, as the parameter is reversed. Of course, computer experiments are not proofs and you should check the numerics carefully before making any firm conclussions.

Finally, you should also be aware of a degenarate Hopf bifurcation. An example is given by the damped pendulum $\ddot{x} + \mu\dot{x} + sinx = 0$. As we change the

damping μ from positive to negative, the fixed point at the origin changes from a stable to an unstable spiral. However at $\mu = 0$ we do not have a true Hopf bifurcation because there are no limit cycles an either side of the bifurcation. Instead at $\mu = 0$ we have a continuous band of closed orbits surrounding the origin. These are not limit cycles! (Recall that a limit cycle is an isolated closed orbit.)

This degenerate case typically arises when a nonconservative system suddenly becomes conservative at the bifurcation point. Then the fixed point becomes a nonlinear center, rather than the weak spiral required by a Hopf bifurcation. **Chapter 8.3 Oscillating Chemical Reactions**
For an application of Hopf bifurcations, we now consider a class of experimental systems known as chemical oscillators. These systems are remarkable, both for their spectacular behavior and for the story behind their discovery. After presenting this backgrounding information, we analyze a simple model proposed recently for oscillations in the chlorine dioxide-iodine-malonic acid reaction. The definitive reference on chemical oscillations is the book edited by Field and Burger (1985). See also Epstein et al. (1983), Winfree (1987b) and Murray (1989). **Belousov's "Supposedly Discovered Discovery"**

In the early 1950s the Russian biochemist Boris Belousov was trying to create a test tube caricature of the Krebs cycle, a metabolic process that occurs in living cells. When he mixed citric acid and bromate ions in a solution of sulfuric acid, and in the presence of a cerium catalyst, he observed to his astonishment that the mixture became yellow, then faded to a colorless again, and continued to oscillate dozens of times before finally reaching equilibrium after about an hour.

Today it comes as no surprise that chemical reactions can oscillate spontaneously - such reactions have become a standard demonstration ini chemistry classes, and you may have seen one yourslef. (For recipes, see Winfree (1980)). But in Belousov's day, his discovery was so radical that he couldn't get his work published. It was thought that all solutions of chemical reagents must go monotonically to equilibrium, because of the laws of thermodynamics. Belousov's paper was rejected by one journal after another. According to Winfree (1987b, p161) one editor even added a snide remark about Belousov's "supposedly discovered dicovery" to the rejection letter.

Belousov finally managed to publish a brief abstract in the obscure proceedings of a Russian medical meeting (Belousov 1959), although his colleagues weren't aware of it until years later. Nevertheless, word of this amazing reaction circulated among Moscow chemists in the late 1950s and in 1961 a graduate student named Zhabotinsky was assigned by his advisor this work to lgiht at an international conference in Prague in 1968, one of the few times that Western and Soviet scientists were allowed to meet. At that time there was a great deal of interest in biological and biochemical oscillations (Chance et al. 1973) and the BZ reaction, as it came to be called, was seen as a manageable model of those more complex systems.

The analogy to biology turned out to be surprisingly close: Zaikin and

Zhabotinsky (1970) and Winfree (1972) observed beautiful propagating waves of oxidation in thin unstirred layers of BZ reagent, and found that these waves annihilate upon collision, just like waves of excitation in neural or cardiac tissue. The waves always take the shape of expanding concentric rings or spirals (Color Plate 1). Spiral waves are now recognized to be a ubiquitous feature of chemical, biological, and physical excitable media; in particular, spiral waves and their three-dimensional analogs, "scroll waves" (Front cover illustration) appear to be implicated in certain cardiac arhythmias, a problem of great medical importance (Winfree 1987b).

Boris Belousov would be pleased to see what he started.

In 1980, he and Zhabotinsky were awarded the Lenin Prize, the Soviet Union's highest medal, for their pioneering work on oscillating reactions. Unfortunately, Belousov had passed away ten years earlier.

For more about the history of the BZ reaction, see Winfree (1984, 1987b). An English translation of Belousov's original paper from 1951 appears in Field and Burger (1985).

Chlorine Dioxide-Iodine-Malonic Acid Reaction

The mechanisms of chemical oscilations can be very complex. The BZ reaction is thought to involve more than twenty elementary reaction steps, but luckily many of them equilibrate rapidly-this allows the kinetics to be reduced to as few as three differential equations. See Tyson (1985) for this reduced system and its analysis.

In a similar spirit, Lengyel et al. (1990) have proposed and analyzed a particularly elegant model of another oscillating reaction, the chlorine dioxide-iodine-malonic acid ($ClO_2 - I_2 - MA$) reaction. Their experiments show that the following three reactions and empirical rate laws capture the behavior of the system:

$$\mathrm{MA} + \mathrm{I_2} \rightarrow \mathrm{IMA} + \mathrm{I^-} + \mathrm{H^+}; \qquad \frac{d[\mathrm{I_2}]}{dt} = -\frac{k_{1a}[\mathrm{MA}][\mathrm{I_2}]}{k_{1b} + [\mathrm{I_2}]} \qquad (1)$$

$$\mathrm{ClO_2} + \mathrm{I^-} \rightarrow \mathrm{ClO_2^-} + \tfrac{1}{2}\mathrm{I_2}; \qquad \frac{d[\mathrm{ClO_2}]}{dt} = -k_2[\mathrm{ClO_2}][\mathrm{I^-}] \qquad (2)$$

$$\mathrm{ClO_2^-} + 4\mathrm{I^-} + 4\mathrm{H^+} \rightarrow \mathrm{Cl^-} + 2\mathrm{I_2} + 2\mathrm{H_2O};$$

$$\frac{d[\mathrm{ClO_2^-}]}{dt} = -k_{3a}[\mathrm{ClO_2^-}][\mathrm{I^-}][\mathrm{H^+}] - k_{3b}[\mathrm{ClO_2^-}][\mathrm{I_2}]\frac{[\mathrm{I^-}]}{u + [\mathrm{I^-}]^2} \qquad (3)$$

Typical values of the concentrations and kinetic parameters are given in Lengyel et al. (1990) and Lengyel and Epstein (1991).

Numerical integrations of (1)-(3) show that the model exhibits oscilla-

tions that closely resemble those observed experimentally. However this model is still too complicated to handle analytically. To simplify it, Lengyel et al. (1990) use a result found in their simulations: Three of the reactants (MA, I_2 and ClO_2) vary much more slowly than the intermediates I^- and CIO_2^-, which change by several orders of magnitude during an oscillation period. By approximating the concentrations of the slow reactants as constants and making other reasonable simplifications, they reduce the system to a two-variable model. (Of course, since this approximation neglects the slow consumption of the reactants, the model will be unable to account for the eventual appraoch to equilibrium). After suitable nondimensionalization, the model becomes

$$\dot{x} = a - x - \frac{4xy}{1+x^2} \qquad 4$$

$$\dot{y} = bx(1 - \frac{y}{1+x^2}) \qquad 5$$

where x and y are the dimensionless concentrations of I^- and CIO_2^-. The parameters $a, b > 0$ depend on the empirical rate constants and on the concentrations assumed for the slow reactants.

We begin the analysis of (4), (5) by constructing a trapping region and applying the Poincare-Bendixson theorem. Then we'll show that the chemical oscillations arise from a supercritical Hopf bifurcation.

Chapter 8.4 Global bifurcation of cycles

In two-dimensional systems, there are four common ways in which limit cycles are created or destroyed. The Hopf bifurcation is the most famous, but the other three deserve their day in the sun. They are harder to detect because they involve large regions of the phase plane rather than just the neighborhood of a single fixed point. Hence they are called global bifurcations. In this section we offer some prototypical examples of global bifurcations, and then compare them to one another and the Hopf bifurcation. A few of their scientific applications are discussed in Sections 8.5 and 8.6 and in the excercises.

Saddle-Node bifurcation of cycles

A bifurcation in which two limit cycles coalesce and annihilate is called a fold or saddle-node bifurcation of cycles, by analogy with the related bifurcation of fixed points. An example occurs in the system

$$\dot{r} = \mu r + r^3 - r^5$$

$$\dot{\theta} = \omega + br^2$$

studied in Section 8.2. There we were interested in the subcritical Hopf bifurcation at $\mu = 0$; now we concentrate on the dynamics for $\mu < 0$

It is helpful to regard the radial equation $\dot{r} = \mu r + r^3 - r^5$ as a one-dimensional system. As you should check, this system undergoes a saddle-node bifurcation of fixed points at $\mu_c = 1/4$. Now returning to the two-dimensional system, these fixed points correspond to circular limit cycles. Figure 8.4.1 plots the "radial phase portraits" and the corresponding behavior in the phase plane

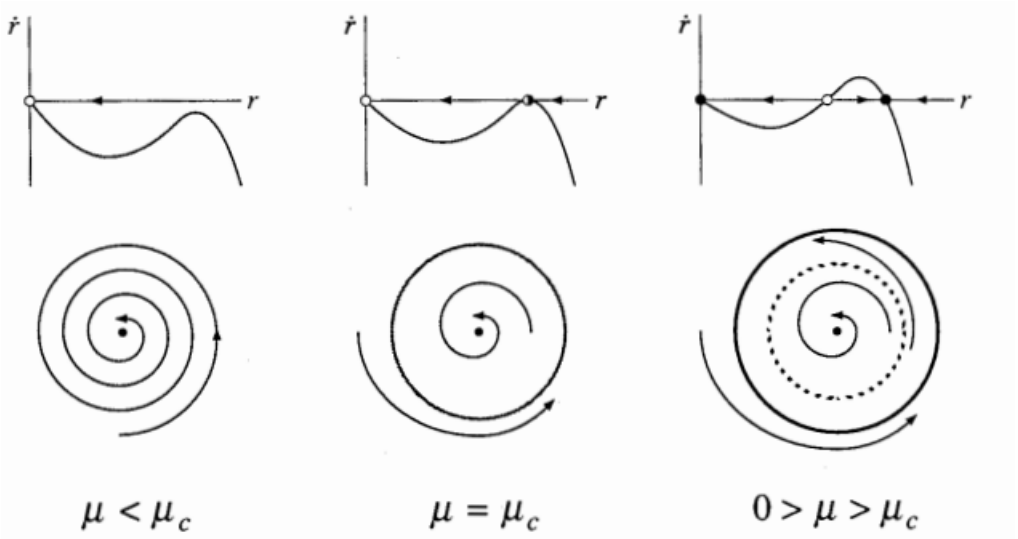

Figure 8.4.1

At μ_c a half-stable cycle is born out of the clear blue sky. As μ increases it splits into a pair of limit cycles, one stable, one unstable. Viewed in other direction, a stable and unstable cycle collide and disappear as μ decreases through μ_c. Notice that the origin remains stable throughout; it does not participate in this bifurcation.

For future reference, note that at birth the cycle has O(1) amplitude, in contrast to the Hopf bifurcation, where the limit cycle has small amplitude proportional to $(\mu - \mu_c)^{1/2}$.

Infinite-period Bifurcation

Consider the system:

$$\dot{r} = r(1 - r^2)$$
$$\dot{\theta} = \mu - sin\theta$$

where $\mu \geq 0$. This system combines two one-dimensional systems that we have studied previously in Chapters 3 and 4. In the radial direction, all trajectories (except $r* = 0$) approach the unit circle monotonically as $t \to \infty$. In this angular direction, the motion is everywhere counterclockwise if $\mu > 1$, whereas there are two invariant rays defined by $sin\theta = \mu$ if $\mu < 1$. Hence as μ decreases through $\mu_c = 1$, the phase portraits change as in Figure 8.4.2

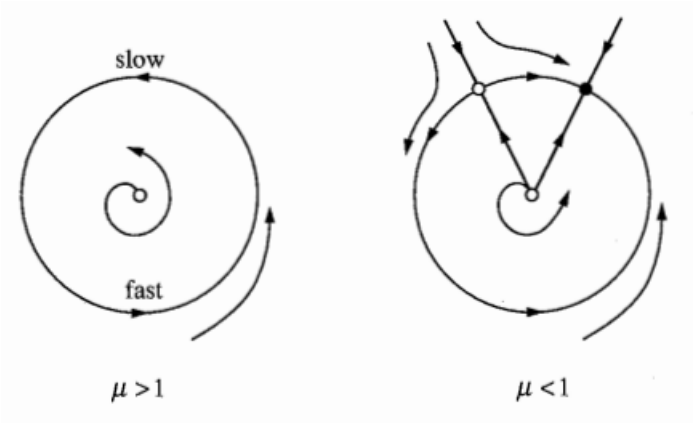

Figure 8.4.2

As μ decreases, the limit cycle r=1 develops a bottleneck at $\theta = \pi/2$ that becomes increasingly severe as $\mu \to 1*$. The oscillations period lengthens and finally becomes infinite at $\mu_c = 1$, when a fixed point appears on the circle; hence the term infinite-period bifurcation. For $\mu < 1$, the fixed point splits into a saddle and a node.

As a bifurcation is approached the amplitude of the oscillation stays O(1) but the period increases like $(\mu - \mu_c)^{-1/2}$, for the reasons discussed in Section 4.3. **Homoclinic Bifurcation**

In this scenario, part of a limit cycle moves closer and closer to a saddle point. At the bifurcation the cycle touches the saddle point and becomes a homoclinic orbit. This is another kind of infinite period bifurcation; to avoid confusion, we'll call it a saddle-loop or homoclinic bifurcation.

It is hard to find an analytically transparrent example, so we resort to the computer. Consider

$$\dot{x} = y$$
$$\dot{y} = \mu y + x - x^2 + xy.$$

Figure 8.4.3 plots a series of phase portraits before, during and after the bifurcation; only the important features are shown.

Numerically, the bifurcation is found to occur at $\mu_c = -0.8645$. For $\mu < \mu_c$, say $\mu = -0.92$, a stable limit cycle passes close to a staddle point at the origin (Figure 8.4.3a). As μ increases to μ_c, the limit cycle swells (Figure 8.4.3b) and bangs into the saddle, creating a homoclinic orbit (Figure 8.4.3c). Once $\mu > \mu_c$, the saddle connection breaks and the loop is destroyed (Figure 8.4.3d)

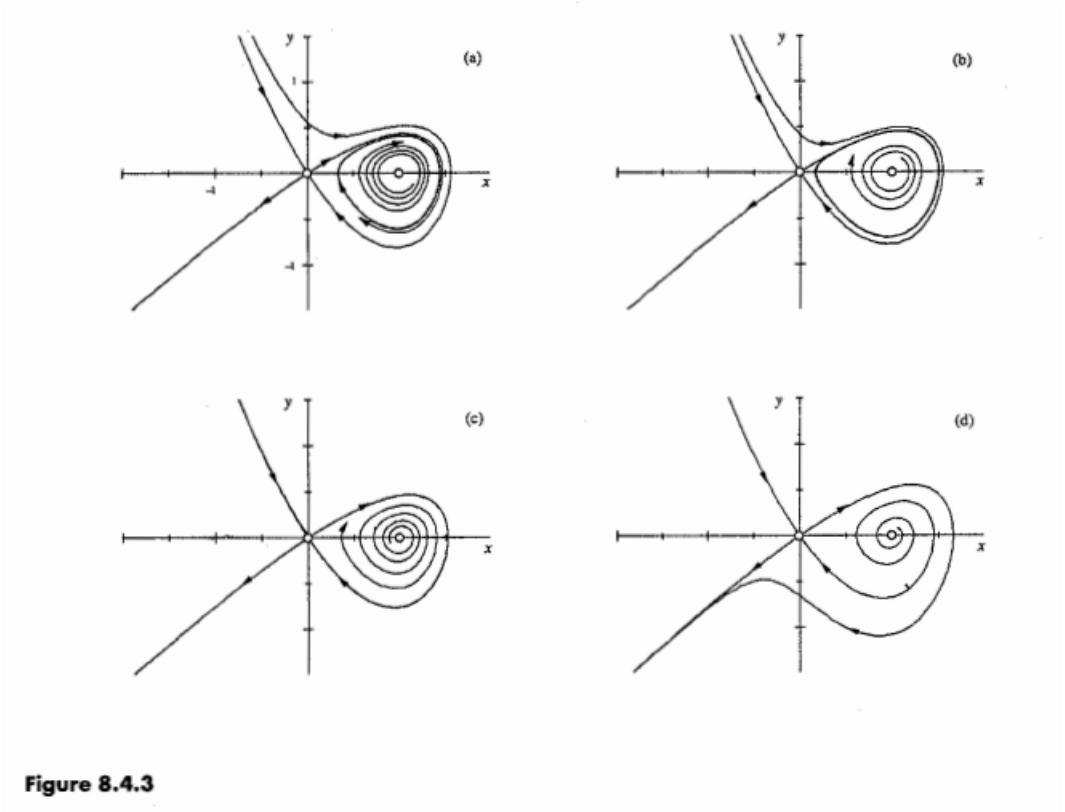

Figure 8.4.3

The key to this bifurcation is the behavior of the unstable manifold of the saddle. Look at the branch of the unstable manifold that leaves the origin to the northeast; after it loops around, it either hits the origin (Figure 8.4.3c) or veers off to one side or the other (Figures 8.4.3a, d). **Scaling Laws**

For each of the bifurcation given here, there are characteristic scaling laws that govern the amplitude and period of the limit cycle as the bifurcation is approached. Let μ denote some dimensionless measure of the distance from the bifurcation and assume that $\mu << 1$. The generic scaling laws for bifurcation of cycles in two-dimensional systems are given in Table 7.4.1

	Amplitude of stable limit cycle	Period of cycle
Supercritical Hopf	$O(\mu^{1/2})$	$O(1)$
Saddle-node bifurcation of cycles	$O(1)$	$O(1)$
Infinite-period	$O(1)$	$O(\mu^{-1/2})$
Homoclinic	$O(1)$	$O(\ln \mu)$

Table 7.4.1

All of these laws have been explained previously, except those for the homoclinic bifurcation. The scaling of the period in that case is obtained by estimating the time required for a trajectory to pass by a saddle point (see Excercise 8.4.12 and Gaspard 1990)

Exceptions to these rules can occur, but only if there is some symmetry or other special feature that renders the problem nongeneric, as in the following example.

Chapter 8.5 Hysteresis in the Driven Pendulum and Josephson Junction

This section deals with a physical problem in which both homoclinic and infinte period bifurcations arise. The problem was introduced back in Sections 4.4 and 4.6. At that time or equivalently, its high tech analog, a superconducting Josephson junction driven by a constant current. Because we weren't ready for two dimensional systems, we reduced both problems to vector fields on the circle by looking at the heavily overdamped limit of negligible mass (for the pendulum) or negligible capacitance (for the Josephson junction)

Now we're ready to tackle the full two-dimensional problem. As we claimed at the end of Section 4.6 for sufficiently weak damping the pendulum and the Josephson junction can exhibit intriguing hysteresis effects, thanks to the coexistence of a stable limit cycle and a stable fixed point. In physical terms, the pendulum can settle into either a rotating solution where it whirls over the top, or a stable real state into either a rotating solution where it whirls over the top, or a stable rest state where gravity balances the applied torque. The final state depends on the initial conditions. Our goal now is to understand how this bistability comes about.

We will phrase our discussion in terms of the Josephson junction, but will mention the pendulum analog whenever it seems helpful. **Governing Equations**

As explained in Section 4.6 the governing equation for the Josephson junction is

$$\frac{\hbar C}{2e}\ddot{\phi} + \frac{\hbar}{2eR}\dot{\phi} + I_c sin\phi = I_B \qquad (1)$$

where $\hbar$ is Plank's constant divided by 2π, e is the charge of the electron, I_B is

the constant bias current, C, R and I_c are the junction's capacitance, resistance, and critical current, and $\phi(t)$ is the phase difference accros the junction.

To highlight the role of damping, we nondimensionalize (1) differently from Section 4.6. Let

$$\tilde{t} = (\frac{2eI_c}{\hbar C})^{1/2}t, \qquad I = \frac{I_B}{I_c}, \qquad \alpha = (\frac{\hbar}{2eI_cR^2C})^{1/2} \qquad (2)$$

Then (1) becomes

$$\phi^{''} + \alpha\phi^{'} + sin\phi = I \qquad (3)$$

where α and I are the dimensionless damping and applied current, and the primed denotes differentiation with respect to $\tilde{t}$. Here $\alpha > 0$ on physical grounds, and we may choose $t \geq 0$ without loss of generality (otherwise, redefine $\phi \to -\phi$).

Let $y = \phi^{'}$. Then the system becomes

$$\phi^{'} = y$$

$$y^{'} = I - sin\phi - \alpha y. \qquad (4)$$

As in Section 6.7 the phase space is a cylinder, since ϕ is an angular variable and y is a real number (best thought of as an angular velocity).

Fixed Points

The fixed points of (4) satisfy $y* = 0$ and $sin\phi* = I$. Hence there are two fixed points on the cylinder if $I < 1$ and none if $I > 1$. When the fixed points exist, one is a saddle and the other is a sink, since the Jacobian $A = \begin{pmatrix} 0 & 1 \\ -cos\phi** & -\alpha \end{pmatrix}$ has $\tau = -\alpha < 0$ and $\triangle = cos\phi* = \pm\sqrt{1-I^2}$. When $\triangle > 0$, we have a stable node if $\tau^2 - 4\triangle = \alpha^2 - 4\sqrt{1-I^2} > 0$, i.e. if the damping is strong enough or if I is close to 1; otherwise the sink spiral. At $I = 1$ the stable node and the saddle coalesce in a saddle-node bifurcation of fixed points. **Existence of a Closed Orbit**

What happens when $I > 1$? There are no more fixed points available; something new has to happen. We claim that all trajectories are attracted to a unique, stable limit cycle.

The first step is to show that a periodic solution exists. The argument uses a clever idea introduced by Poincare long ago. Watch carefully-this idea will come up frequently to our later work.

Consider the nullcline $y = \alpha^{-1}(I - sin\phi)$ where $y^{'} = 0$. The flow is downward above the nullcline and upward below it (Figure 8.5.1)

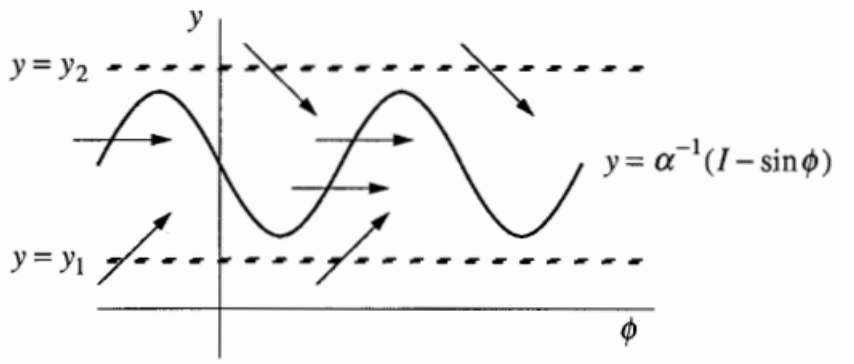

Figure 8.5.1

In particular, all trajectories eventually enter the strip $y_1 \leq y \leq y_2$ (Figure 8.5.1), and stay in there forever. (Hence y_1 and y_2 are any fixed numbers such that $0 < y_1 < (I-1)/\alpha$ and $y_2 > (I+1)/\alpha$). Inside the strip, the flow is always to the right because $y > 0$ implies $\phi^{'} > 0$
Also, since $\phi = 0$ and $\phi = 2\pi$ are equivalent on the cylinder, we amy as well confine our attention to the rectangular box $0 \leq \phi \leq 2\pi$, $y_1 \leq y \leq y_2$. This box contains all the information about the long term behavior of the flow (figure 8.5.2).

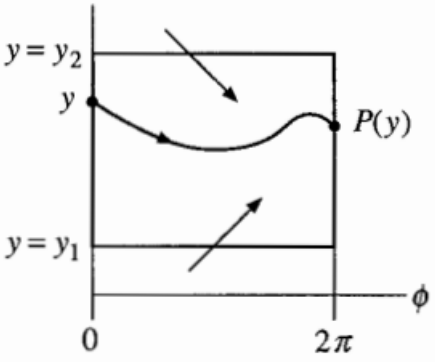

Figure 8.5.2

Now consider a trajectory that starts at a height y on the left side of the box, and follow it until it intersects the right side of the box at some new height P(y), as shown in Figure 8.5.2. The mapping from y to P(y) is called the Poincare map. it tells us how the hieght of a trajectory changes after one lap around the cylinder (figure 8.5.3).

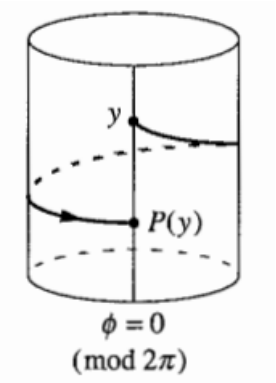

Figure 8.5.3

The Poincare map is also called the first return map, because if a trajectory starts at a height y on the line $\phi = 0(\text{mod } 2\pi)$, then P(y) is its height when it returns to that line for the first time.

Now comes the key point: we cant compute P(y) explicitly but if we can show that there's a point y* such that P(y*)=y*, then the corresponding trajectory will be a closed orbit (because it returns to the same location on the cylinder after one lap).

To show that a y* must exist, we need to know what the graph of P(y) looks like at least roughly. Consider a trajectory that starts at $y = y_1, \phi = 0$. We claim that

$$P(y_1 > y_1$$

This follows because the flow is strictly upward at first, and the trajectory can never return to the line $y = y_1$, since the flow everywhere upward on that line (recall Figures 8.5.1 and 8.5.2). By the same kind of argument,

$$P(y_2) < y_2$$

Furthermore, P(y) is a continuous function. This follows from the theorem that solutions of differential equations depend continuously on initial conditions, if the vector field is smooth enough.

And finally, P(y) is a monotonic funciotn (By drawing pictures, you can convince yourself that if P(y) were not monotonic; two trajectories would cross- and that's forbidden). Taken together, these results imply that P(y) has the shape shown in Figure 8.5.4

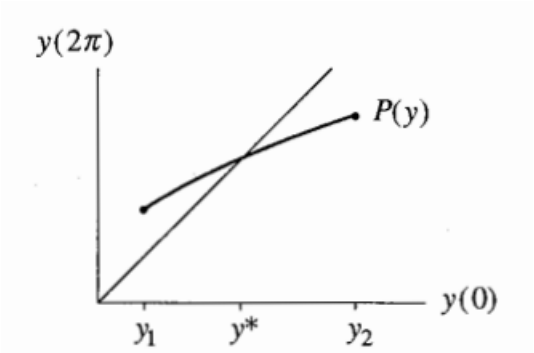

Figure 8.5.4

By the intermediate value theorem (or common sense), the graph of P(y) must cross the 45° diagonal somewhere, that intersection is our desired y*.

Uniqueness of the Limit Cycle

The argument above proves the existence of a closed orbit, and almost proves its uniqueness. But we haven't excluded the possibilities that P(y)=y on some interval in which case there would be a band or infinitely many closed orbits.

To nail down the uniqueness part of our claim, we recall from Section 6.7 that there are two topologically different kinds of periodic orbits on a cylinder: liberations and rotations (Figure 8.5.5).

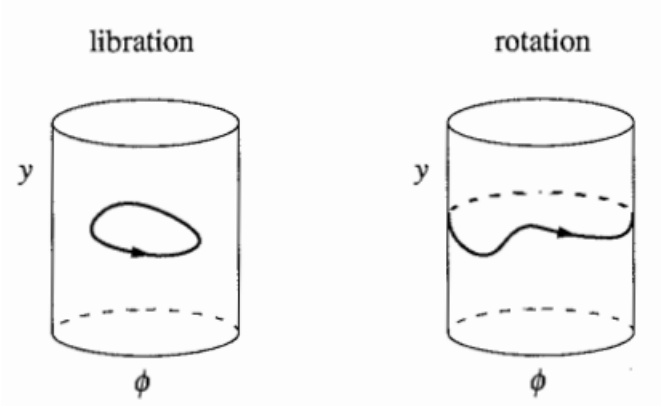

Figure 8.5.5

For $I > 1$, liberations are impossible because any liberation must encircle a fixed point, by index theory-but there are no fixed points when $I > 1$. Hence we only need to consider rotations.

Suppose that were two different rotations. The phase portrait on the cylinder would have to look like Figure 8.5.6

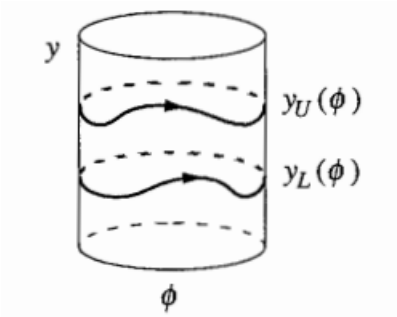

Figure 8.5.6

One of the rotations would have to lie strictly above the other because trajectories can't cross. Let $y_U(\phi)$ and $y_L(\phi)$ denote the "upper" and "lower" rotations, where $y_U(\phi) > y_L(\phi)$ for all ϕ.

The existence of two such rotations leads to a contradiction, as shown by the following energy argument. Let

$$E = \frac{1}{2}y^2 - cos\phi \qquad (5)$$

After one circuit around any rotation $y(\phi)$, the change in energy $\triangle E$ must vanish. Hence

$$0 = \triangle E = \int_0^{2\pi} \frac{dE}{d\phi} d\phi \qquad (6)$$

But (5) implies

$$\frac{dE}{d\phi} = y\frac{dy}{d\phi} + sin\phi \qquad (7)$$

and

$$\frac{dy}{d\phi} = \frac{y'}{\phi'} = \frac{I - sin\phi - \alpha y}{y} \qquad (8)$$

From (4). Substituting (8) into (7) gives $dE/d\phi = I - \alpha y$. Thus (6) implies

$$0 = \int_0^{2\pi} (I - \alpha y) d\phi$$

on any rotation $y(\phi)$. Equivalently, any rotation must satisfy

$$\int_0^{2\pi} y(\phi) d\phi = \frac{2\pi I}{\alpha} \qquad (9)$$

But since $y_u(\phi) > y_L(\phi)$,

$$\int_0^{2\pi} y_U(\phi) d\phi > \int_0^{2\pi} y_L(\phi) d\phi,$$

and so (9) can't hold for both rotations.

This contradiction proves that the rotation for $I > 1$ is unique, as claimed.

Homoclinic Bifurcation

Suppose we slowly decrease I, starting from some value $I > 1$. What happens to the rotating solution? Think about the pendulum: as the driving torque is reduced value $I_c < I$, the torque is insufficient to overcome gravity and damping and the pendulum can no longer whirl. Then the rotation disappears and all solutions damp out to the rest state.

Our goal now is to visualize the corresponding bifurcation in phase space. In Excecise 8.5.2, you're asked to show (by numerical computation of the phase portrait) that if α is sufficiently small, the stable limit cycle is destroyed in a homoclinic bifurcation (Section 8.4). The following schematic drawings summa-

rize the results you should get.

First suppose $I_c < I < 1$. The system is bistable: a sink coexists with a stable limit cycle (Figure 8.5.7).

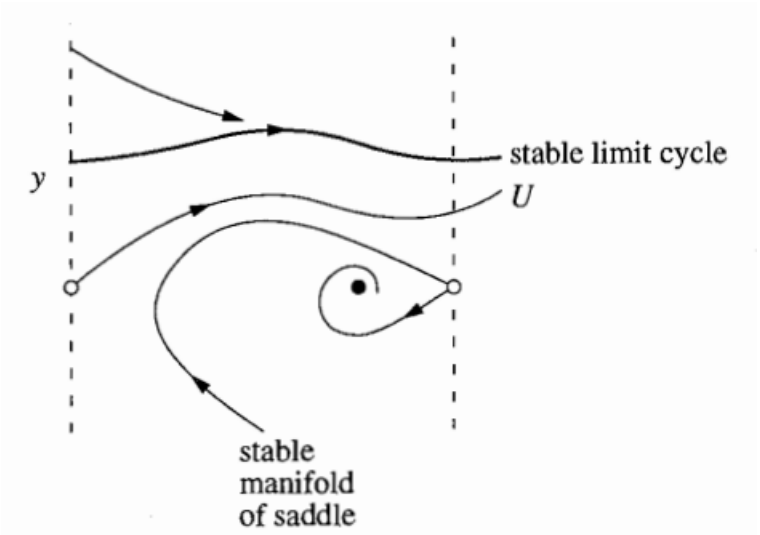

Figure 8.5.7

Keep your eye on the trajectory labeled U in Figure 8.5.7. It is a branch of the unstable manifold of the saddle. As $t \to \infty$, U asymptotically appraoches the stable limit cycle.

As I decreases, the stable limit cycle moves down and squezes U closer to the stable manifold of the saddle. When $I = I_c$, the limit cycle merges with U in a homoclinic bifurcation. Now U is a homoclinic orbit - it joins the saddle to itself (Figure 8.5.8).

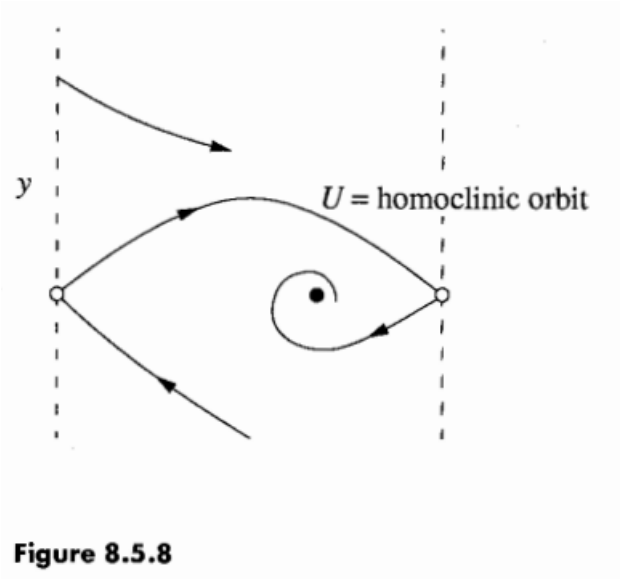

Figure 8.5.8

Finally, when $I < I_c$, the saddle connection breaks and U spirals into the sink (Figure 8.5.9).

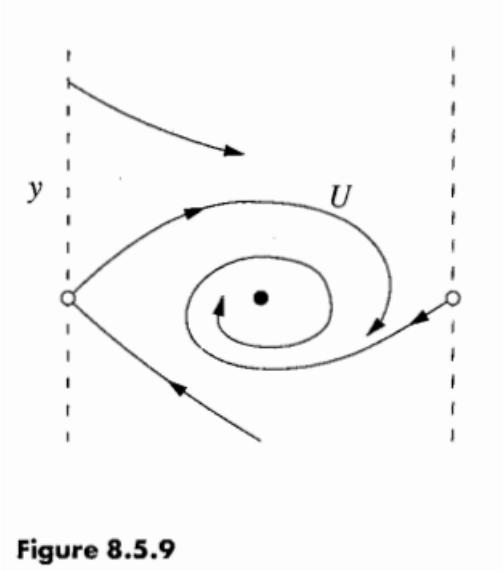

Figure 8.5.9

The scenario described here is valid only if the dimensionless damping α is sufficiently small. We know that something different has to happen for large α. After all, when α is infinite we are in the overdamped limit studied in Section 4.6. Our analysis there showed that the periodic solution is destroyed by an infinite periodic bifurcaiton (a saddle and a node are born on the former limit cycle). So it's plausible that an infinite-period bifurcation should also occur if α is large but finite. These intuitive ideas are

confirmed by a numerical integration (Excercise 8.5.2).
Putting it all together, we arrive at the stability diagram shown in FIgure 8.5.10. Three types of bifurcations occur: homoclinic and infinite period bifurcations of periodic orbits, and a saddle-node bifurcation of fixed points.

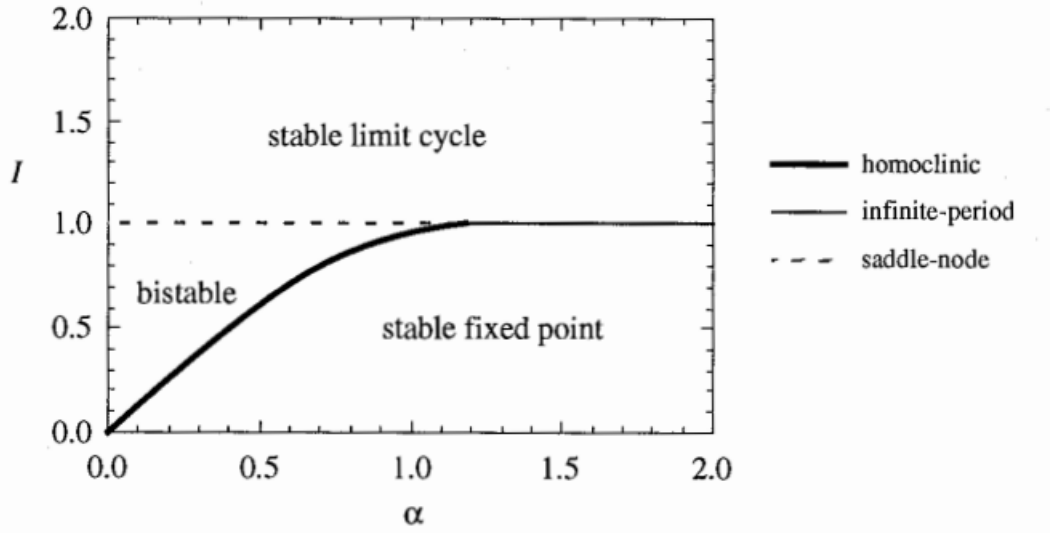

Figure 8.5.10

Our argument leading to Figure 8.5.10 has been heuristic. For rigorous proofs, see Levi et al (1978). Also Guckenheimer and Holmes (1983, p 202) derive an analytical approximation for the homoclinic bifurcation curve for $\alpha << 1$, using an advanced technique known as Meinkov's method. They show that the bifurcation curve is tangent to the line $I = 4\alpha/\pi$ as $\alpha \to 0$. Even if α is not so small, this approximation works nicely, thanks to the straightness of the homoclinic bifurcation curve in Figure 8.5.10. **Hysteretic Current-Voltage Curve**

Figure 8.5.10 explains why lightly damped Josephson junctions have hysterectic I-V curves. Suppose α is small and I is initially below the homoclinic bifurcation (thick line in Figure 8.5.10). Then the junction will be operating at the stable fixed point, corresponding to the zero-voltage state. As I is increased, nothing changes until I exceeds 1. Then the stable fixed point disappears in a saddle node bifurcation, and the junction jumps into a nonzero voltage state (the limit cycle).

If I is brought back down, the limit cycle persists below I=1 but its frequency tends to zero continuously as I_c is approached. Specifically, the frequency tends to zero like $[ln(I - I_c)]^{-1}$, just as expected from the scaling law discussed in Section 8.4. Now recall from Section 4.6 that the junction's dc-voltage is proportional to it's oscillation frequency. Hence, the voltage also returns to zero continuously as $I \to I_c*$ (Figure 8.5.11).

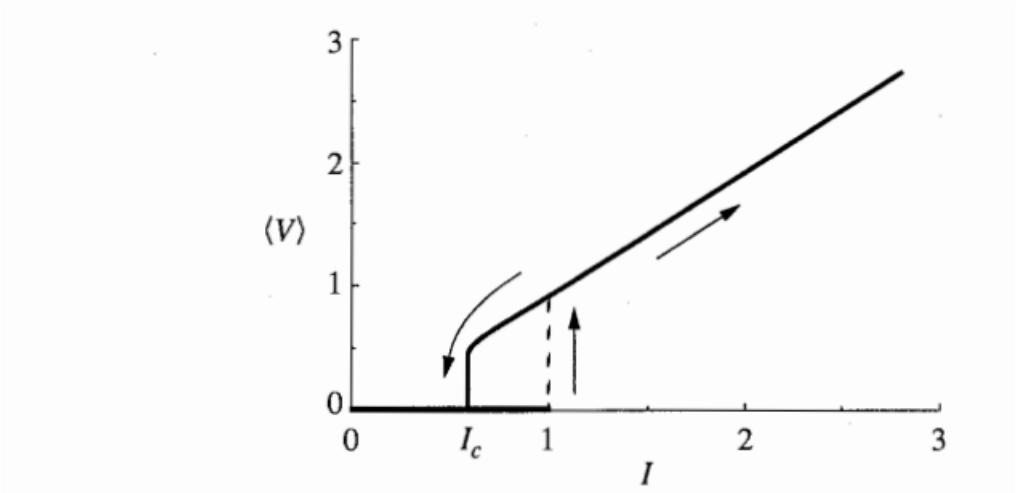

Figure 8.5.11

In practice, the voltage appears to jump discontinuously back to zero, but that is to be expected because $[ln(I - I_c)]^{-1}$ has infinite derivatives at all orders at I_c! (See excercise 8.5.1) The steepness of the curve makes it impossible to resolve the continuous return to zero. For instance, in experiments on pendula, Sullivan and Zimmerman (1971) measured the mechanical analog of the I-V curve - namely, the curve relating the rotation rate to the applied torque. Their data show a jump back to zero rotation at the bifurcation.

Chapter 8.6 Coupled Oscillations and Quasiperiodicity

Besides the plane and the cylinder, another important two-dimensional phase space is the torus. It is the natural phase space for systems of the form

$$\dot{\theta}_1 = f_1(\theta_1, \theta_2)$$
$$\dot{\theta}_2 = f_2(\theta_1, \theta_2)$$

where f_1 and f_2 are periodic in both arguments.

For instance, a simple model of coupled oscillators is given by

$$\dot{\theta}_1 = \omega_1 + K_1 sin(\theta_2 - \theta_1)$$
$$\dot{\theta}_2 = \omega_2 + K_2 sin(\theta_2 - \theta_1), \qquad (1)$$

where θ_1, θ_2 are the phases of the oscillators, $\omega_1, \omega_2 > 0$ are their natural frequencies, and $K_1, K_2 \geq 0$ are coupling constants. Equation (1) has been used to model the interaction between human circadian rhythms and the sleep-wake cycle (Strogratz 1986, 1987).

An intuitive way to think about (1) is to imagine two friends jogging on a circular track. Here $\theta_1(t), \theta_2(t)$ represent their positions on the track, and ω_1, ω_2 are proportional to their preferred running speeds. If they were uncoupled, then each would run at his or her preferred speed and the faster one would periodically overtake the slower one (as in Example 4.2.1). But these are friends-they want

to run around together! So they need to compromise, with each adjusting his or her speed as necessary. If their preferred speeds are too different, phase-locking will be impossible and they may want to find new running partners.

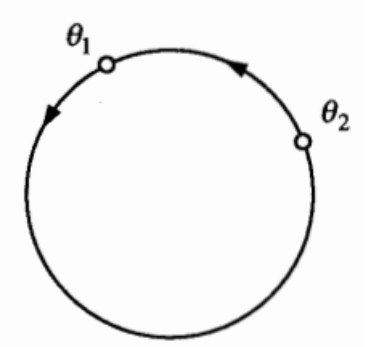

Figure 8.6.1

Here we consider (1) more abstractly, to illustrate some general features of flows on the torus and also to provide in example of a saddle node bifurcation of cycles (Section 8.4). To visualize the flow, imagine two points running around a circle at instantaneous rates $\dot{\theta}_1$, $\dot{\theta}_2$ (Figure 8.6.1). Alternatively, we could imagine a single point tracing out a trajectory on a torus with coordinates θ_1, θ_2 (Figure 8.6.2). The coordinates are analogous to lattitude and logitude.

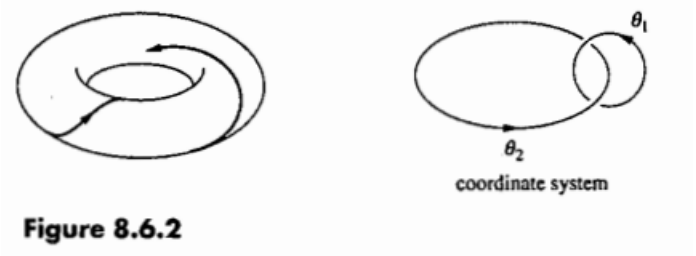

Figure 8.6.2

But since the curved surface of a torus makes it hard to draw phase portraits, we prefer to use an equivalent representation: a square with periodic boundary conditions. Then if a trajectory runs off an edge, it magically reappears on the opposite edge, as in some video games (Figure 8.6.3).

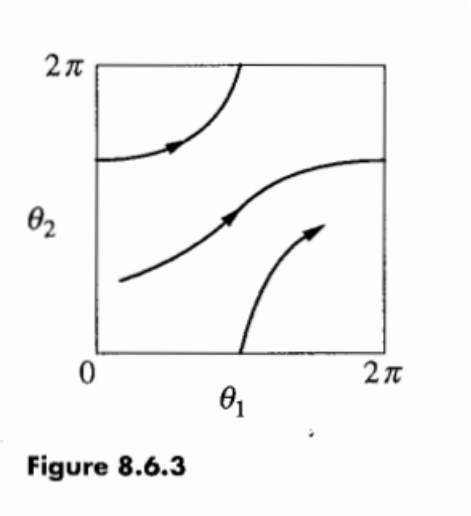

Figure 8.6.3

Uncoupled System

Even the seemingly trivial case of uncoupled oscillators ($K_1, K_2 = 0$) holds some surprise. Then (1) reduces to $\dot{\theta}_1 = \omega_1, \dot{\theta}_2 = \omega_2$. The corresponding trajectories on the square are straight lines with constant slope $d\theta_2/d\theta_1 = \omega_2/\omega_1$. There are two qualitatively different cases, depending on whether the slope is a rational or irrational number.

If the slope is rational, then $\omega_1/\omega_2 = p/q$ for some integers p, q with no common factors. In this case all trajectories are closed on the torus, because θ_1 completes p revolutions in the same time that θ_2 complete q revolutions. For example, Figure 8.6.4 shows a trajectory on the square with p=3, q=2.

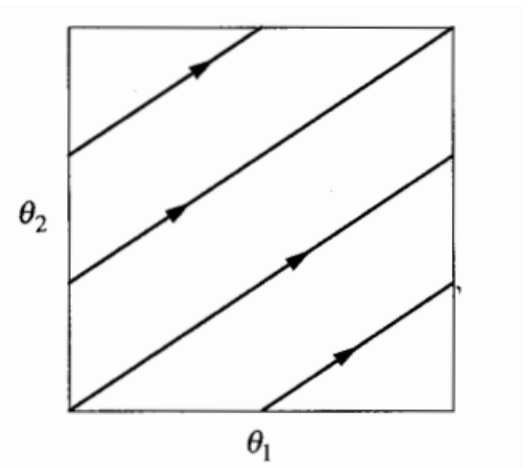

Figure 8.6.4

When plotted on the torus the trajectory gives ... a trefoil knot! Figure 8.6.5 shows a trefoil, alongside a top view of a torus with a trefoil wound around it.

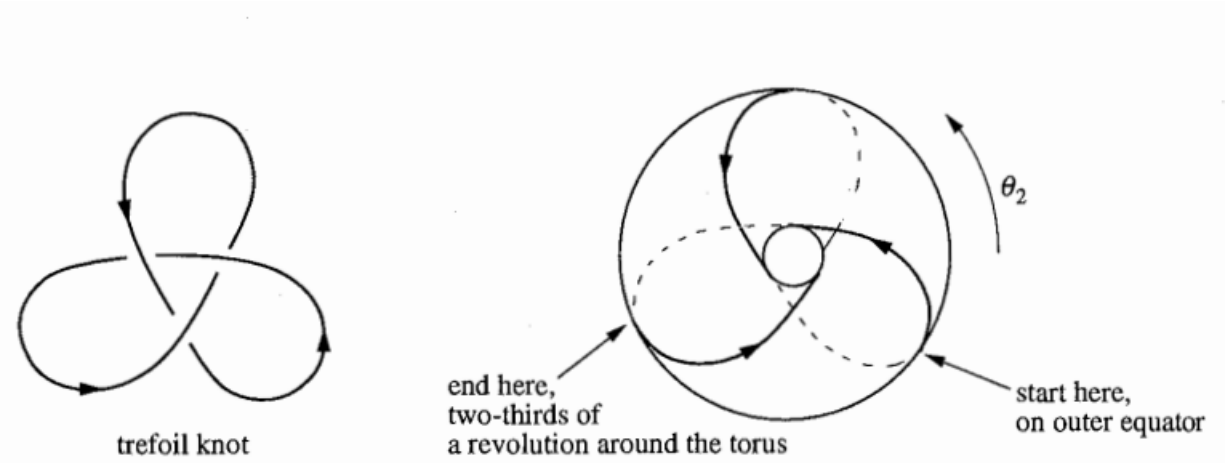

Figure 8.6.5

Do you see why this knot corresponds to p=3, q=2? Follow the knotted trajectory in FIgure 8.6.5 and count the number of revolutions made by θ_2 during the time that θ_1 makes one revolution, where θ_1 is latitude and θ_2 is longitude. Starting on the outer equator, the trajectory moves onto the top surface, dives into the hole, travels along the bottom surface, and then reappears on the outer equator, two-thirds of the way around the torus. Thus θ_2 makes two-thirds of a revolution while θ_1 makes one revolution; hence p=3, q=2.

In fact, the trajectories are always knotted if p, $q \geq 2$ have no common factors. The resulting curves are called p:q torus knots.

The second possibility is that the slope is irrational (Figure 8.6.6). Then the flow is said to be quasiperiodic. Every trajectory winds around endlessly on the torus, never intersecting itself and yet never quite closing.

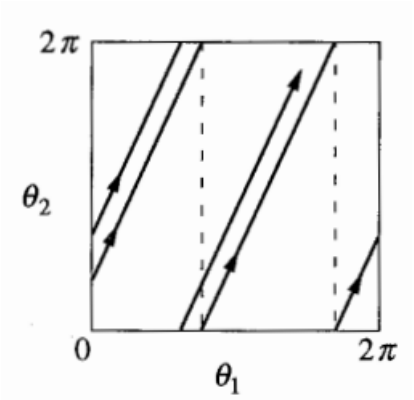

Figure 8.6.6

How can we be sure the trajectories never close? Any closed trajectory encessarily makes an integer number of revolutions in both θ_1 and θ_2; hence the slope would have to be rational, contrary to assumption.
Furthermore, when the slope is irrational, each trajectory is dense on the torus: in other words, each trajectory comes arbitrarily close (Excercise 8.6.3).

Quasiperiodicity is significant because it is a new type of long-term behavior. Unlike the earlier entries (fixed point, closed orbit, homoclinic and heteroclinic orbits and cycles), quasiperiodicity occurs only on the torus.

Coupled System

Now consider (1) in the coupled case where $K_1, K_2 > 0$. The dynamics can be deciphered by looking at the phase difference $\phi = \theta_1 - \theta_2$. Then (1) yields 4 different types of plates. Look toward page 277.

Chapter 8.7 Poincare Maps

In Section 8.5 we used a Poincare map to prove the existence of a periodic orbit for the driven pendulum and Josephson Junction. Now we discuss Poincare maps more generally.

Poincare maps are useful for studying swirling flows, such as the flow near a periodic orbit (or as we'll see later, the flow in some chaotic system). Consider an n-dimensional system $\dot{x} = f(x)$. Let S be an n-1 dimenionsal surface of section (Figure 8.7.1). S is required to be transverse to the flow, i.e., all trajectories starting on S flow through it, not parallel to it.

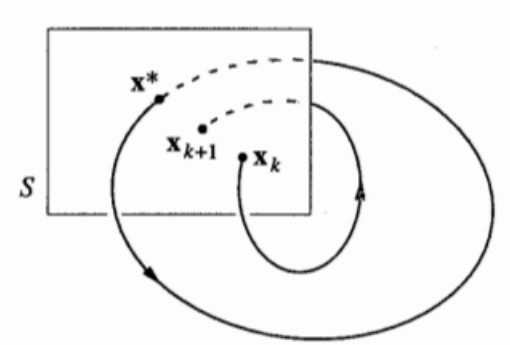

Figure 8.7.1

The Poincare map P is a mapping from S to itself, obtained by following trajectories from one intersection with S to the next. If $x_1 \in S$ denotes the kth intersection, then the Poincare map is defined by

$$x_{k+1} = P(x_k).$$

Suppose that x* is a fixed point of P, i.e., P(x*)=x*. Then a trajectory starting at x* returns to x* after some time T, and is therefore a closed orbit for the original system $\dot{x} = f(x)$. Moreover, by looking at the behavior of P near this fixed point, we can determine the stability of the closed orbit.

Thus the Poincare map converts problems about closed orbits (which are difficult) into problems about fixed points of a mapping (which are easier in principle though not always in practice). The snag is that it's typically impossible to find a formula for P. For the sake of illustration, we begin with two examples for which P can be computed explicitly.

Linear Stability of Periodic Orbits

Now consider the general case: Given a system $\dot{x} = f(x)$ with a closed orbit, how can we tell whether the orbit is stable or not? Equivalently, we ask whether the corresponding fixed point x* of the Poincare map is stable. Let v_0 be an infinitiesimal pertubation such that $x* + v_0$ is in S. Then after the first return to S,

$$\begin{aligned} x* + v_1 &= P(x* + v_0) \\ &= P(x*) + [DP(x*)]v_0 + O(||v_0||^2) \end{aligned}$$

where DP(x*) is an (n-1)x(n-1) matrix called the linearized Poincare map at x*. Since x*=P(x*), we get

$$v_1 = [DP(x*)]v_0$$

assuming that we can neglect the small $O(||v_0||^2)$ terms.

The desired stability criterion is expressed in terms of the eigenvalues λ, of DP(x*): The closed orbit is linear stable if and only if $|\lambda_j| < 1$ for all $j = 1, ..., n-1$.

To understand this criterion, consider the generic case where there are no repeated eigenvalues. Then there is a basis of eigenvectors $\{e_j\}$ and so we can write $v_0 = \sum_{j=1}^{n-1} v_j e_j$ for some scalars v_j. Hence

$$v_1 = (DP(x*)) \sum_{j=1}^{n-1} v_j e_j = \sum_{j=1}^{n-1} v_j \lambda_j e_j.$$

Iterating the linearized map k times gives

$$v_k = \sum_{j=1}^{n-1} v_j (\lambda_j)^k e_j.$$

Hence, if all $|\lambda_j| < 1$, then $||v_k|| \to 0$ geometrically fast. This proves that x* is linearly stable. Conversely, if $|\lambda_j| > 1$ for some j, then pertubations along e_j grow, so x* is unstable. A borderline case occurs when the largest eigenvalue has magnitude $|\lambda_m| = 1$; this occurs at bifurcations of periodic orbits, and then a nonlinear stability analysis is required.

The λ_j are called the characteristic or Floquet multipliers of the periodic orbit. Strictly speaking, these are the nontrivial multipliers; there is always an additional trivial multiplier $\lambda = 1$ corresponding to pertubations along the periodic orbit. We have ignored such pertubations since they just amount to time-translation).

In general, the characteristic multipliers can only be found by numerical integration (see Excercise 8.7.10). The following examples are two of the rare exceptions.